Journal of Current Science and Technology, September-December 2022 Vol. 12 No. 3, pp. 417-427

ISSN 2630-0656 (Online)

Cite this article: Rajnaveen, B., Naik, D. B., Rambabu, G., & Rao, K. S. (2022, September). Optimization of electron beam welding parameters to improve corrosion resistance of AA2219 aluminium alloy. *Journal of Current Science and Technology, 12*(3), 417-427. DOI:

Journal of Current Science and Technology

Journal homepage: https://jcst.rsu.ac.th

Optimization of electron beam welding parameters to improve corrosion resistance of AA2219 aluminium alloy

B Rajnaveen[1*], D Balaji Naik[2], G Rambabu[1], and K Srinivasa Rao[1]

[1]Department of Mechanical Engineering, Andhra University, Visakhapatnam, India-530003
[2]Department of Mechanical Engineering, Universal College of Eng. & Tech, Guntur India-52200

*Correspondence; E-mail: rajnaveenb@gmail.com

Received 12 February 2022; Revised 22 May 2022; Accepted 26 May 2022;
Published online 26 December 2022

Abstract

Aluminium alloys are ideal for the production of lightweight structures. These alloys also have a high strength-to-weight ratio and superior corrosion resistance. Electron beam welding (EBW) is widely used for the joining of AA2219 al alloy, which is a high-energy beam welding technology that melts the workpiece surface and forms the joint using a focused beam of electrons. The Taguchi method of experimental design was applied in this study to examine the effect of input parameters on corrosion resistance. Input parameters like welding current, travel speed and voltage are used as controlling parameters to create the experimental design, and each parameter is divided into three levels. Therefore, an L9 orthogonal array was used for the experimental design. Potentio dynamic polarization tests were conducted for all designed experimental arrays to determine the pitting potential (corrosion resistance) in millivolts. An Analysis of Variance (ANOVA) technique was used to determine the governing parameters of the process. The findings of ANOVA revealed that voltage is the most influential parameter, followed by welding current and travel speed. Further, response surface methodology (RSM) has been used to form the mathematical model of the AA2219 aluminium alloy. This mathematical model helped in finding the predicted value of pitting potential. The optimized parameters of the AA2219 aluminium alloy were obtained by using RSM. The outcomes of RSM indicate that maximum corrosion resistance is achieved when welding current, travel speed and voltage are chosen as 50 mA, 1200 mm/min and 53 kV respectively.

Keywords: *AA2219 alloy; corrosion resistance; electron beam welding; response surface methodology; travel speed; voltage; welding current.*

1. Introduction

For aircraft applications, aluminium alloys are the most commonly used materials. Various aluminium alloys can be used to make riveted structural parts that meet certain needs, like high strength and high damage tolerance. However, the necessity to reduce aircraft weight and manufacturing costs have prompted the development of dynamically strengthened metallic structures (Heinz et al., 2000; Dursun, & Soutis, 2014; Rambabu, Eswara Prasad, Kutumbarao, & Wanhill, 2017; Verma, & Lila, 2021; Grbović, Burzić, & Perković, 2022; Kumar & Singh, 2022). Improved precipitation-hardened aluminium alloys such as Al-Cu, Al-Mg-Si, and Al-Zn-Mg have been developed as another key option for weight reduction. AA2219, which has 6.03% Cu, 0.23% Mn, 0.11% Zr, 0.09% V, and 0.06% Ti, was made in 1954 and has mostly replaced the AA2025 alloy. In addition to its high strength-to-weight ratio and

excellent cryogenic qualities, the AA2219 alloy offers a wide strength range. Liquid cryogenic rocket fuel tanks are most commonly constructed with the AA2219 alloy (Banerjee, Bhadra, & Gogoi, 2020). However, the rate of corrosion of the welded plates of such al-alloy welds is higher (lower corrosion resistance) than the reference base material. Corrosion attacks are more localized, as may be seen. The samples are perforated in several areas, indicating poor corrosion resistance. Hence, the pitting potential characteristic of aluminium alloys in the electron beam (EB) welds becomes a serious issue (Koona, Ramana, Prasad, & Vikas, 2021; Jebaraj, Aditya, Kumar, Ajaykumar, & Deepak, 2020; Naik, Rao, Rao, Reddy, & Rambabu, 2019). The galvanic coupling caused by variations in electrochemical potentials between the matrix, precipitates, and intermetallics of the base metal is widely regarded as the primary cause of weld (Sriba, & Vogt, 2021). As intermetallics with copper has different electrochemical properties than the matrix, they make the metal less resistant to corrosion in seawater (Srinivasa Rao, & Prasad Rao, 2006).

Extensive studies have been done on electron beam welded AA2219 alloy, particularly on optimization of parameters as well as the evaluation of mechanical properties (Brennecke, 1965; Trzil, & Hood, 1969). It has been discovered that copper distribution within the matrix is more uniform in electron beam welds, resulting in better mechanical properties (Rao, Reddy, Rao, Kamaraj, & Rao, 2005). The Grey Relation Method is being utilized (Sobih, Elseddig, Almazy, & Sallam, 2016) to optimise the EBW parameters for the 2219 Al-Alloy in terms of yield strength, bead shape and hardness. The appropriate combination of EBW parameters improves the performance attributes of the EBW process, such as yield tensile strength, hardness, penetration depth, and bead width. Despite superior mechanical properties, electron beam welded joints also suffer from fusion welding defects (Wang et al., 2021). However, the addition of copper to aluminium improves its overall strength, but it has a significant negative impact on the metal's corrosion resistance. The surface of metallic copper is highly efficient at reducing oxygen, and therefore, copper-rich sites allow oxygen and proton reduction reactions to occur with enhanced efficiency, thus increasing the probability of stable pit growth (Xu, & Liu, 2009). Furthermore, the microstructure and different welding parameters have a significant effect on how corrosion works (Yang et al., 2020). During electron beam welding, the fusion zone has a finer grain size because of rapid cooling rates in the weld zone (Mastanaiah, Sharma, & Reddy, 2018).

As there is not much published information on the statistically significant effect on pitting corrosion of electron beam welded AA2219 al-alloy, and it is very essential to study the effect of welding parameters on corrosion resistance, the present work is aimed at the statistical significance and optimization of welding parameters to improve the corrosion resistance.

2. Objective

The main objective of the present work is to improve the corrosion resistance of electron beam welded AA2219 aluminium alloy by optimizing the welding parameters employing response surface methodology. This can be accomplished by developing a suitable regression model which relates the responses and welding parameters. The present work also aimed to study the effect of individual parameters that influence corrosion resistance.

3. Methodology

3.1 Material and methods

The material used in the present investigation was high strength AA2219 aluminium alloy in T87 temper condition of size 310 mm x 150 mm x 7 mm and is procured from Vision Castings & Alloys Pvt Ltd in Hyderabad. The elemental composition of AA2219 is given in Table 1. The plates were longitudinally butt welded by using electron beam welding machine as shown in Figure 1. The joint produced is an autogenous butt weld without a single square groove. The samples were prepared for corrosion testing after the welding process. The method used for design of experiments is Taguchi design. This design employs orthogonal arrays to analyze the effects of variables on the mean and variation of the response. Response surface method (RSM) was used for optimize the process design which gives a best approximation of the true response surface over a factor region.

Figure 1 EBW weld joint

Table 1 Elemental Composition (%Wt.) of parent metal AA2219-T87 Al-alloy

Material	Cu	Mg	V	Fe	Si	Ti	Mn	Zr	Al
AA2219	6.08	0.01	0.09	0.10	0.07	0.06	0.23	0.11	93.2

3.2 Pitting corrosion test

Pitting corrosion behaviour of AA2219 alloy welds was determined using Gill AC potentiostat and is shown in Figure 2. 3.5% NaCl solution was used for all the pitting corrosion experiments with standard electrodes of calomel and pure graphite (ASTM G107). Potential scan speed of 0.166 mVs^{-1}, pH of 10 and exposure area of 1 cm^2 were used and the potential at which sudden increase in current occurs is considered as critical pitting potential. Better pitting resistance is indicated by the higher positive potential value. Potentio dynamic polarization curves are obtained upon testing to correlate the pitting corrosion resistance

Figure 2 Basic Electrochemical System for corrosion testing (Gill AC)

3.3 Taguchi and RSM

3.3.1 Taguchi design

Taguchi design with systematic data is more likely to be obtained via a well-planned set of experiments, in which all relevant parameters are adjusted over a pre-determined range. The selected ranges of each parameter shown defect free welds which are observed from radiography tests. However, the fact that process characteristics are being presented is typical and understandable due to the nature of the welding process as well as some preliminary experiments based on the machine capabilities to obtain defect-free welds.

Table 2 Parameters and levels

S. no	Parameter	Notation	Unit	Levels		
				1	2	3
1	Welding current	WC	mA	30	40	50
2	Travel speed	WS	mm/min	800	1000	1200
3	Voltage	WV	kV	40	50	60

The ranges of electron beam welding parameters were studied to construct a mathematical (regression) equation for corrosion resistance values. Table 2 lists the EBW parameters and their respective levels. Table 3 shows the Taguchi L_9 orthogonal array for three parameters each one at three levels. Using the design of experiments and RSM in Mini-tab software, a mathematical equation was created utilizing Table 3 as input data.

Table 3 Design matrix with experimental results

Experiment Number	Parameters			Corrosion Pit Potential (mV)
	WC	WS	WV	
1	30	800	40	-581
2	30	1000	50	-535
3	30	1200	60	-510
4	40	800	50	-490
5	40	1000	60	-525
6	40	1200	40	-570
7	50	800	60	-482
8	50	1000	40	-560
9	50	1200	50	-455

3.3.2 RSM

RSM is indeed a set of statistical and mathematical approach for modelling and analyzing the events in which the desired response is influenced by several variables, with the goal of optimizing that response. The response (Corrosion resistance) can be defined as a function of welding current (WC), travel speed (WS) and voltage (WC)

Corrosion resistance (CR) = f (WC, WS, WV)

The response CR is expressed by using regression equation

CR = -523.3 - 3.917 WC - 1.708 WS +
47.67 WV + 0.075 WC*WC +
0.0750 WS*WS - 0.40 WV*WV +
0.005 WC*WS - 0.10 WC*WV (1)

Equation (1) represents regression equation for corrosion resistance expressed as a function of input factors. Main and interaction effects are considered for each parameter. The parameters are tested at 95% confidence level for their significance by using Minitab software package. It is possible to calculate the R^2 (coefficient of correlation) to see how well an experimental value fits a predetermined value. (Rekab, & Shaikh, 2005; Anderson, & McLean, 2018). The R^2 value, in this case, is 0.94, indicating that the model only explains 1% of all variances.

3.3.3 Contour and response surface plots

In the evaluation of the response surface, contour plots are extremely useful. The experimenter can readily characterize the form of the surface and determine the optimum with reasonable precision by developing contour plots for response surface analysis using Minitab software.

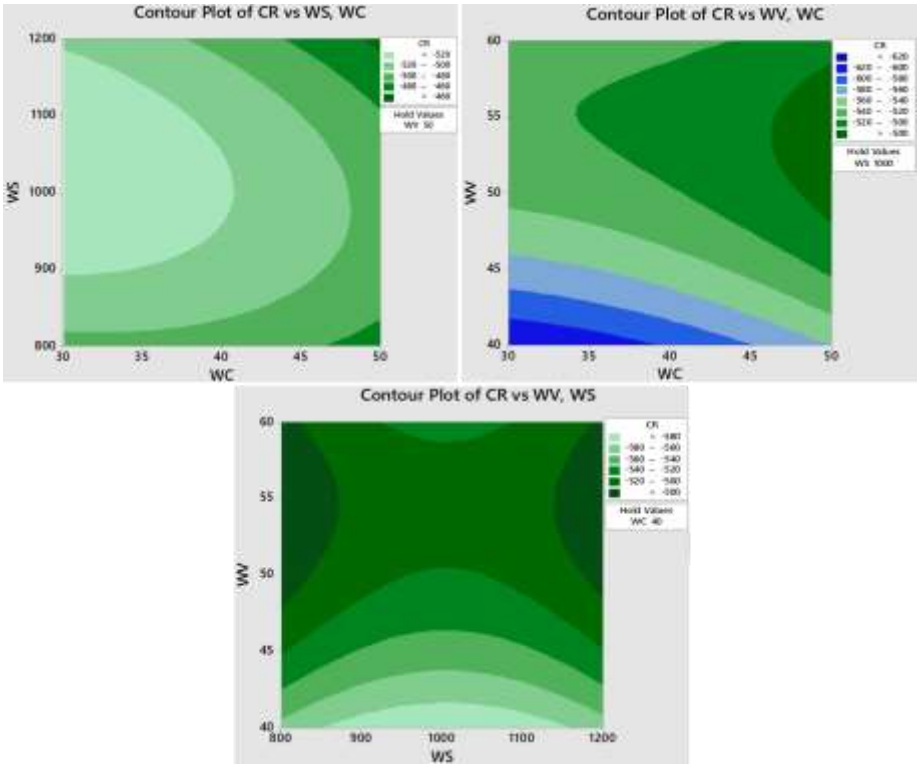

Figure 3 Contour plot for CR

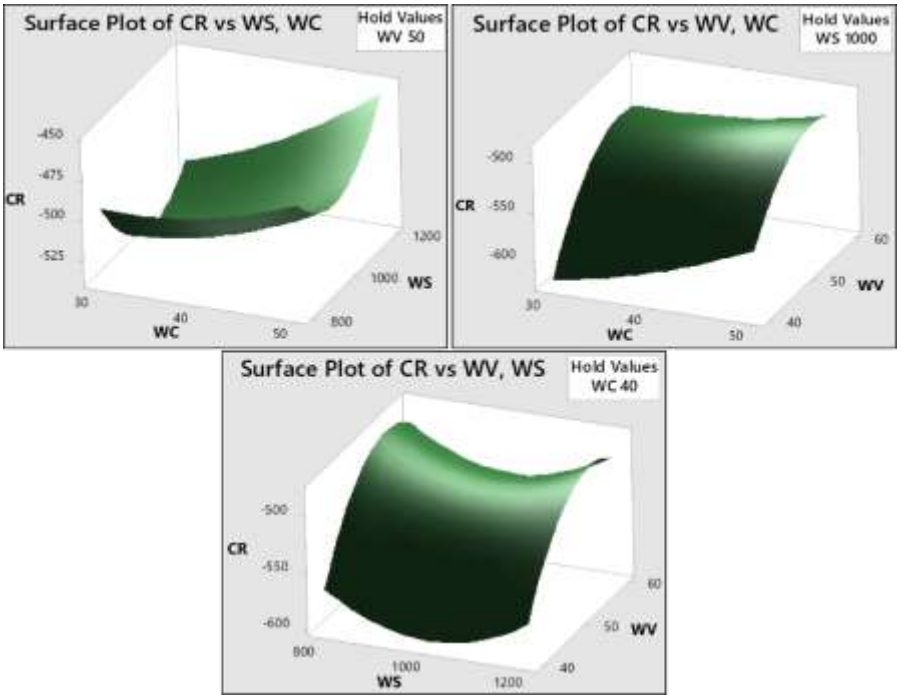

Figure 4 Surface plot for CR

In most cases**,** the contour plots are two-dimensional and sometimes they are three-dimensional also. These plots can be drawn with Minitab software by varying two parameters while the other is held constant. Figure 3 represents contour plots for corrosion resistance which depicts the variation among the welding factors and there is significant interaction exist between voltage and welding current. When the voltage and welding current increases, heat input during welding also increases which causes improved corrosion resistance. The study of a response surface is analogous to "climbing a hill" to find the maximum response (Montgomery, 2017). The response surface plots for corrosion resistance are obtained as shown in Figure 4. These plots depict the optimum welding conditions at apex for electron beam welding process to achieve maximum corrosion resistance. It is also observed that there exists nonlinear (higher order) variation between the welding factors on corrosion resistance.

4. Results and discussion

4.1 Microstructure of fusion zone

It has been assumed that the most of second phase particles (θ) are dissolved during fusion welding by leaving only a few particles in the weld metal when the process is completed. However, not all of them are dissolved in EBW because of the high cooling rates involved. The optical micrographs of the fusion zone in AA2219-T87 electron beam welds are depicted in Figure 5. As illustrated in Figure 5, fine grains were discovered in the fusion zone of EB welds. Chen, Miao, Li, and Lin (2009), Nair, Phanikumar, Prasad Rao, and Sinha (2007) make similar observations regarding grain size in the fusion zone. Because of the extremely high solidification rates associated with electron beam welding, the fine dendritic structure is observed in EB welds. Also, the formation of solidification cracking in fusion zone was observed with higher voltage values (Figure 5(5)).

At grain boundaries, AA2219 Al-alloys are anodic to matrix and dissolution occurs (Trishul, & Panda, 2020). Chain of precipitates at grain boundaries establishes galvanic coupling with the matrix and causes pitting corrosion. The corrosion behavior of the EBW weld zone is expected to be different from corrosion in the base metal, and this may affect the long-term structural integrity of the EB welded material. Specifically, the microstructural variations in the different EBW zones are expected to produce galvanic effects that may induce localized corrosion, such as pitting (Majeed, Mehta, & Siddiquee, 2021). The poor pitting corrosion resistance (PCR) in the weld zone of as welded sample may be attributed to the partial dissolution of precipitates during EBW. The randomly oriented deformed grains and the remaining un-dissolved precipitates cause the pit initiation. Pitting occurs as a result of local matrix dissolution caused by galvanic interaction between intermetallics and the surrounding matrix. When the passive layer on the material's surface is damaged, it causes a massive discharge of electrons thereby a sudden rise in current (Figure 6). The potential at which the current increases drastically was considered as critical pitting potential (E_{pit}) (Esmailzadeh, Aliofkhazraei, & Sarlak, 2018) which is observed in potentio dynamic polarization curves as shown in Figure 7. This E_{pit} value is the criterion for evaluating corrosion resistance.

4.2 ANOVA analysis of variance

The most significant welding parameters that affect the corrosion resistance of EBW AA2219 material were identified using analysis of variance (ANOVA). The ANOVA results are shown in Tables 4. The results of ANOVA indicate that WV is the process parameter that has a significant contribution to the corrosion resistance values of EBW AA2219 material. In addition, a regression model by Minitab has been developed. The P-value of welding voltage is 0.019 which is the most significant factor whereas the travel speed has a P-value of 0.132, indicating that it should be a less significant factor at the 95 % level of confidence. In this case, WV (voltage) is the most effective parameter which effects the corrosion resistances of AA2219 aluminium alloy. It is also observed that corrosion resistance increases with the decrease in voltage. The control variables are not significant if the P value is higher than 0.1. The "Predicted R-Squared" of 0.98 agrees with the "Adjusted R Squared" of 0.94 in a good fitness of the model.

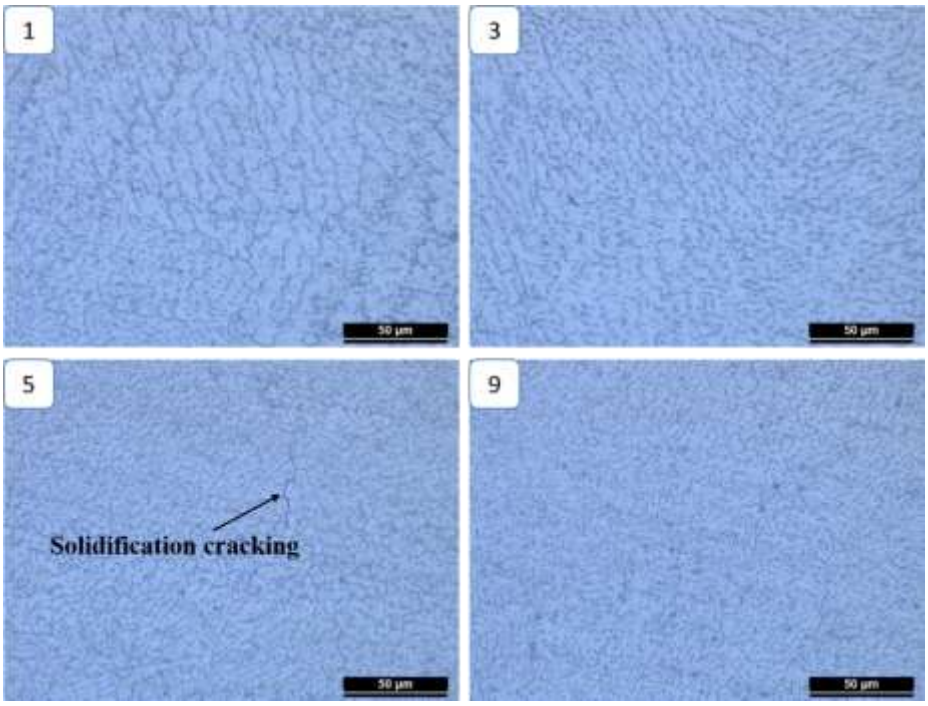

Figure 5 Optical microstructures of EBW AA2219 weld samples for experimental runs 1, 3, 5 and 9 respectively.

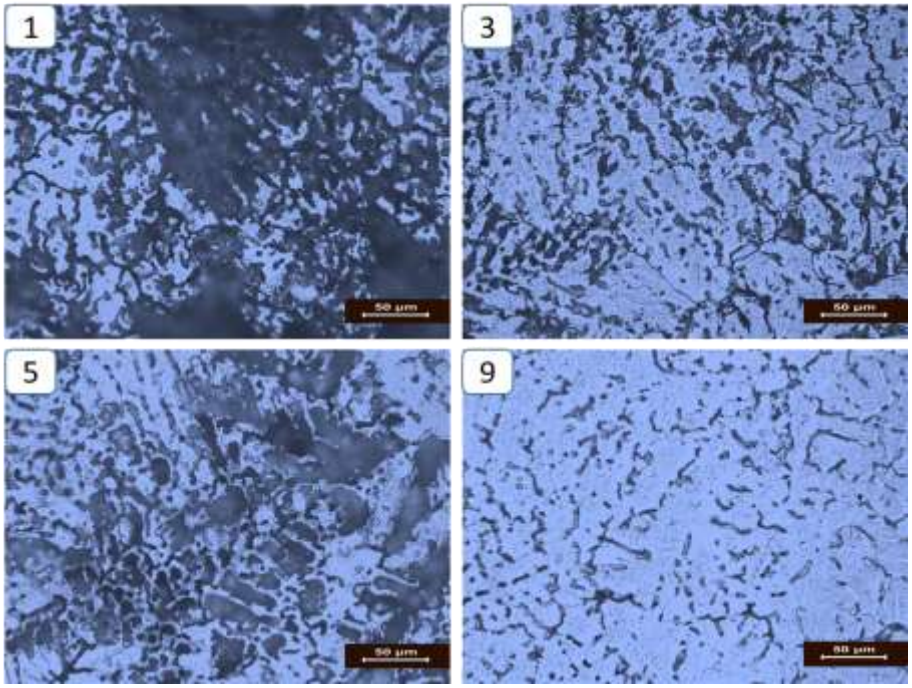

Figure 6 Optical microstructures of EBW AA2219 corroded samples for experimental runs 1, 3, 5 and 9 respectively.

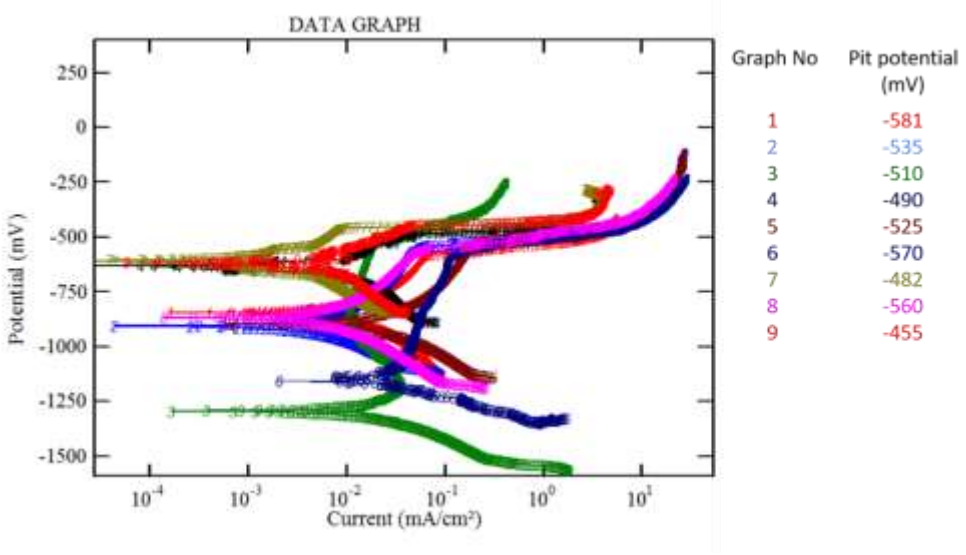

Figure 7 Potentio dynamic polarization curves of AA2219-T87 EB welds.

Table 4 ANOVA results

Source	DOF	Sum of squares	Mean square	F value	P value
WC	2	2716.7	1358.3	13.58	0.069
WS	2	1316.7	658.3	6.58	0.132
WV	2	10066.7	5033.3	50.33	0.019

4.3 Response optimization

From table 5, the optimum value of corrosion resistance -450.55 is obtained at welding current (WC) 50 mA, travel speed (WS) 1200 rpm and voltage (WV) is 53.33 kV respectively. The response optimizer plot in Figure 8 also indicates the optimized welding parameters for maximum corrosion resistance of AA2219 aluminium alloy EB welds. Three confirmation experiments were conducted at optimum welding conditions to validate the predicted corrosion resistance. The results shown that the percentage error between predicted and experimental is in acceptable range which validates the improved corrosion resistance at optimal welding parameters.

Table 5 Response Optimization

Solution	WC	WS	WV	CR	Desirability
1	50.0000	1200	53.3333	-450.556	0.98023
2	50.0000	1200	59.1917	-464.284	0.92573
3	50.0000	800	53.7213	-467.282	0.90174
4	50.0000	800	57.2244	-473.278	0.85377
5	30.0000	800	58.3630	-482.282	0.78175
6	30.8333	1200	55.2381	-502.262	0.62190
7	30.4860	1200	55.7696	-502.550	0.61960
8	30.0000	800	40.0000	-580.000	0.42360

Optimal Variable Setting

WC	= 6mm
WS	= 1200 rpm
WV	= 65 mm/min
Corrosion resistance	= -450.56 mV (Predicted)
Corrosion resistance (avg of three)	= -453 mV (Experimental validation)
% of error	= 0.6% (Acceptable)

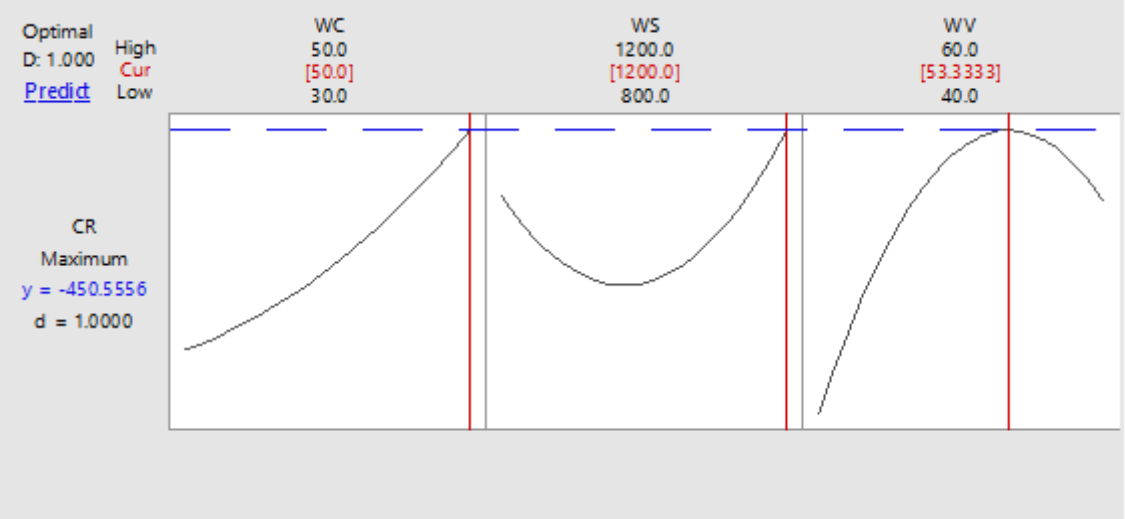

Figure 8 Response Optimizer

5. Conclusions

1. From the ANOVA results the most significant parameter is welding current whereas travel speed is least significant on the corrosion resistance of AA2219 aluminium alloy.
2. Microstructure study revealed that finer dendritic structure because of extremely high solidification rates associated with electron beam welding.
3. Using RSM, the developed regression model was able to predict the corrosion resistance of EBW of AA2219 at 95% confidence level.
4. The response surface and contour graphs shown the significant variation among the factors and optimum conditions of EB welds for improved corrosion resistance.
5. The optimum values of EBW process parameters for maximum corrosion resistance are welding current 50 mA, travel speed 1200 rpm and voltage is 53.33 kV respectively.

6. Acknowledgements

Authors express their gratitude to the Department of Metallurgical Engineering, Andhra University, Visakhapatnam for their kind help in conducting welding experiments.

7. References

Anderson, V. L., & McLean, R. A. (2018). *Design of experiments: a realistic approach*. US: CRC Press. https://doi.org/10.1201/9781315141039

Banerjee, S., Bhadra, R., & Gogoi, S. (2020). Investigating Weldability in Microalloyed Al Alloys. In *Advances in Mechanical Engineering* (pp. 271-279). Singapore: Springer. https://doi.org/10.1007/978-981-15-0124-1_25

Brennecke, M. W. (1965). Electron beam welded heavy gage aluminum alloy 2219. Retrieved form https://ntrs.nasa.gov/citations/19650033282

Chen, Y. B., Miao, Y. G., Li, L. Q., & Lin, W. U. (2009). Joint performance of laser-TIG double-side welded 5A06 aluminum alloy. *Transactions of Nonferrous Metals*

Society of China, *19*(1), 26-31. https://doi.org/10.1016/S1003-6326(08)60223-X

Dursun, T., & Soutis, C. (2014). Recent developments in advanced aircraft aluminium alloys. *Materials & Design (1980-2015)*, *56*, 862-871. https://doi.org/10.1016/j.matdes.2013.12.002

Esmailzadeh, S., Aliofkhazraei, M., & Sarlak, H. (2018). Interpretation of cyclic potentiodynamic polarization test results for study of corrosion behavior of metals: a review. *Protection of metals and physical chemistry of surfaces*, *54*(5), 976-989. https://doi.org/10.1134/S207020511805026X

Grbović, A., Burzić, Z., & Perković, S. (2022). Influence of Corrosion on Parameters of Fracture Mechanics of Aluminium Alloys 2024-T351 and 7075-T651. *Tehnički vjesnik*, *29*(1), 239-245. https://doi.org/10.17559/TV-20210425222503

Heinz, A., Haszler, A., Keidel, C., Moldenhauer, S., Benedictus, R., & Miller, W. S. (2000). Recent development in aluminium alloys for aerospace applications. *Materials Science and Engineering: A*, *280*(1), 102-107. https://doi.org/10.1016/S0921-5093(99)00674-7

Jebaraj, A. V., Aditya, K. V. V., Kumar, T. S., Ajaykumar, L., & Deepak, C. R. (2020). Mechanical and corrosion behaviour of aluminum alloy 5083 and its weldment for marine applications. *Materials Today: Proceedings*, *22*, 1470-1478. https://doi.org/10.1016/j.matpr.2020.01.505

Koona, B., Ramana, V. V., Prasad, C., & Vikas, K. S. R. (2021). Comparison of microstructure and corrosion behaviour of AA2014 electron beam and friction stir welds. *Materials Today: Proceedings*, *52*, 1615-1621. https://doi.org/10.1016/j.matpr.2021.11.272

Kumar, R., & Singh, N. K. (2022). Modelling and Simulation on Behaviours of Aluminium Alloys. In *Advances in Mechanical and Materials Technology* (pp. 703-711). Springer, Singapore. https://doi.org/10.1007/978-981-16-2794-1_62

Majeed, T., Mehta, Y., & Siddiquee, A. N. (2021). Precipitation-dependent corrosion analysis of heat treatable aluminum alloys via friction stir welding, a review. *Proceedings of the Institution of Mechanical Engineers, Part C: Journal of Mechanical Engineering Science*, *235*(24), 7600-7626. https://doi.org/10.1177/0954406221100360 9

Mastanaiah, P., Sharma, A., & Reddy, G. M. (2018). Process parameters-weld bead geometry interactions and their influence on mechanical properties: A case of dissimilar aluminium alloy electron beam welds. *Defence technology*, *14*(2), 137-150. https://doi.org/10.1016/j.dt.2018.01.003

Montgomery, D. C. (2017). *Design and analysis of experiments*. New Jersey, US: John wiley & sons.

Naik, D. B., Rao, C. V., Rao, K. S., Reddy, G. M., & Rambabu, G. (2019). Optimization of friction stir welding parameters to improve corrosion resistance and hardness of AA2219 aluminum alloy welds. *Materials Today: Proceedings*, *15*, 76-83. https://doi.org/10.1016/j.matpr.2019.05.027

Nair, B. S., Phanikumar, G., Prasad Rao, K., & Sinha, P. P. (2007). Improvement of mechanical properties of gas tungsten arc and electron beam welded AA2219 (Al–6 wt-% Cu) alloy. *Science and Technology of Welding and Joining*, *12*(7), 579-585. https://doi.org/10.1179/174329307X227210

Rambabu, P. P. N. K. V., Eswara Prasad, N., Kutumbarao, V. V., & Wanhill, R. J. H. (2017). Aluminium alloys for aerospace applications. *Aerospace materials and material technologies*, 29-52. https://doi.org/10.1007/978-981-10-2134-3_2

Rao, S. K., Reddy, G. M., Rao, K. S., Kamaraj, M., & Rao, K. P. (2005). Reasons for superior mechanical and corrosion

properties of 2219 aluminum alloy electron beam welds. *Materials characterization*, *55*(4-5), 345-354. https://doi.org/10.1016/j.matchar.2005.07.006

Rekab, K., & Shaikh, M. (2005). *Statistical design of experiments with engineering applications* (Vol. 252). Boca Raton, FL: Taylor & Francis.

Sobih, M., Elseddig, Z., Almazy, K., & Sallam, M. (2016). Experimental Evaluation and Characterization of Electron Beam Welding of 2219 AL-Alloy. *Indian Journal of Materials Science*, *2016*. https://doi.org/10.1155/2016/5671532

Sriba, A., & Vogt, J. B. (2021). Galvanic Coupling Effect on Pitting Corrosion of 316L Austenitic Stainless Steel Welded Joints. *Metals and Materials International*, *27*(12), 5258-5267. https://doi.org/10.1007/s12540-020-00789-4

Srinivasa Rao, K., & Prasad Rao, K. (2006). Corrosion resistance of AA2219 aluminium alloy: electrochemical polarisation and impedance study. *Materials science and technology*, *22*(1), 97-104. https://doi.org/10.1179/174328406X79405

Trishul, M. A., & Panda, B. (2020). A Review on the Challenges in Welding of Aluminium AA2219 Alloy. *Advances in Lightweight Materials and Structures*, *8*, 663-671. https://doi.org/10.1007/978-981-15-7827-4_68

Trzil, J. P., & Hood, D. W. (1969). Electron Beam Welding 2219-Aluminum Alloy for Pressure Vessel Applications. *Welding Journal*, *48*(9), S395.

Verma, R. P., & Lila, M. K. (2021). A short review on aluminium alloys and welding in structural applications. *Materials Today: Proceedings*, *46*, 10687-10691. https://doi.org/10.1016/j.matpr.2021.01.447

Wang, J., Liu, Z., Bai, S., Cao, J., Zhao, J., Luo, L., & Li, J. (2021). Microstructure evolution and mechanical properties of the electron-beam welded joints of cast Al–Cu–Mg–Ag alloy. *Materials Science and Engineering: A*, *801*, 140363. https://doi.org/10.1016/j.msea.2020.140363

Xu, W., & Liu, J. (2009). Microstructure and pitting corrosion of friction stir welded joints in 2219-O aluminum alloy thick plate. *Corrosion Science*, *51*(11), 2743-2751. https://doi.org/10.1016/j.corsci.2009.07.004

Yang, M., Lu, J., Chen, J., Li, Y., Liu, Y., & Yang, H. (2020). Effect of welding speed on microstructure and corrosion resistance of Al–Li alloy weld joint. *Materials and Corrosion*, *71*(2), 300-308. https://doi.org/10.1002/maco.201911068